Journal: Earth and Planetary Science Letters

Fire and ecosystem change in the Arctic across the Paleocene-Eocene Thermal Maximum

Elizabeth H. Denis[1,a,*], Nikolai Pedentchouk[2], Stefan Schouten[3,4], Mark Pagani[5,+], and Katherine H. Freeman[1]

[1]*Department of Geosciences, The Pennsylvania State University, Deike Building, University Park, PA 16802, USA*
[2]*University of East Anglia, School of Environmental Sciences, Norwich, UK*
[3]*Royal Netherlands Institute for Sea Research (NIOZ), Department of Marine Microbiology and Biogeochemistry, P.O. Box 59, 1790 AB, Den Burg (Texel), the Netherlands*
[4]*Department of Earth Sciences, Utrecht University, Utrecht, the Netherlands*
[5]*Department of Geology and Geophysics, Yale University, PO Box 208109, New Haven, Connecticut 06520, USA*
[a]*Present address: Chemical and Biological Signature Sciences, Pacific Northwest National Laboratory, P.O. Box 999, MSIN P7-50, 902 Bataille Boulevard, Richland, WA 99352, USA*
[+]*Deceased November 17, 2016*
**Corresponding author: ehdenis@gmail.com*

Abstract[1]

Fire has been an important component of ecosystems on a range of spatial and temporal scales. Fire can affect vegetation distribution, the carbon cycle, and climate. The relationship between climate and fire is complex, in large part because of a key role of vegetation type. Here, we evaluate regional scale fire-climate relationships during a past global warming event, the Paleocene-Eocene Thermal Maximum (PETM), in order to understand how vegetation influenced the links between climate and fire occurrence in the Arctic region. To document concurrent changes in climate, vegetation, and fire occurrence, we evaluated biomarkers,

[1]Abbreviations: carbon isotope excursion (CIE); cyclisation of branched tetraether (CBT); dichloromethane (DCM); glycerol dialkyl glycerol tetraether (GDGT); mass spectrometer (MS); mean annual temperature (MAT); methylation of branched tetraether (MBT); Paleocene-Eocene Thermal Maximum (PETM); polycyclic aromatic hydrocarbon (PAH); pristane (Pr); phytane (Ph); total lipid extract (TLE); total organic carbon (TOC)

including polycyclic aromatic hydrocarbons (PAHs), terpenoids, and alkanes, from the PETM interval at a marine depositional site (IODP site 302, the Lomonosov Ridge) in the Arctic Ocean.

Biomarker, fossil, and isotope evidence from site 302 indicates that terrestrial vegetation changed during the PETM. The abundance of the C_{29} *n*-alkanes, pollen, and the ratio of leaf-wax *n*-alkanes relative to diterpenoids all indicate that proportional contributions from angiosperm vegetation increased relative to that from gymnosperms. These changes accompanied increased moisture transport to the Arctic and higher temperatures, as recorded by previously published proxy records. We find that PAH abundances were elevated relative to total plant biomarkers throughout the PETM, and suggest that fire occurrence increased relative to plant productivity. The fact that fire frequency or prevalence may have increased during wetter Arctic conditions suggests that changes in fire occurrence were not a simple function of aridity, as is commonly conceived. Instead, we suggest that the climate-driven ecological shift to angiosperm-dominated vegetation was what led to increased fire occurrence. Potential increases in terrestrial plant biomass that arose from warm, wet, and high CO_2 conditions were possibly attenuated by biomass burning associated with compositional changes in the plant community.

Keywords

Paleocene-Eocene Thermal Maximum (PETM); polycyclic aromatic hydrocarbon (PAH); fire; angiosperms; organic carbon; Arctic

1. Introduction

Many climate modeling studies predict increases in wildfire activity in future decades associated with globally warming climates and shifting hydrologic patterns. Even so,

mechanisms controlling fire patterns are complex and the primary controls are not always clear (Hessl, 2011). Today, increased atmospheric CO_2 concentrations, higher temperatures, and longer dry seasons are associated with increases in fire activity in the western USA (Westerling, 2006). However, shifts in vegetation (e.g., type, abundance, structure, and continuity) can override the influence of warmer and drier conditions (Higuera et al., 2014). In addition, most empirical evidence, which is also the basis of many models, covers centennial scales (or less), and may not readily translate to climate-vegetation-atmospheric CO_2 relationships recorded in the paleorecord on 1,000 to 10,000 year scales (Hessl, 2011). Records of fire occurrence during past major warming events, such as the Paleocene-Eocene Thermal Maximum (PETM), can potentially elucidate fire dynamics during abrupt and extreme warming, and provide insights relevant to anticipating climate, vegetation, and fire associations under future climate scenarios.

The PETM was a geologically abrupt period of global warming that occurred approximately 55.5 million years ago (Westerhold et al., 2012). This climatic event is widely invoked as a geologic analog for modern climate change, even though modern carbon release (~10 Pg C/yr) may be 10 times faster (Cui et al., 2011). The hyperthermal event is marked by a negative carbon isotope excursion (CIE), signifying a major perturbation to the carbon cycle (McInerney and Wing, 2011, and references therein). At least 3,000 Pg of ^{13}C-depleted carbon was released into the atmosphere over ~10,000 years and global temperatures rose ~5-8°C over ~170,000 years (Cui et al., 2011; McInerney and Wing, 2011; Peterse et al., 2012; Sluijs et al., 2006; Weijers et al., 2007; Wing et al., 2005). Concurrently, there were dramatic shifts in vegetation and precipitation patterns around the world (Kraus and Riggins, 2007; Pagani et al., 2006; Wing et al., 2005; Wing and Currano, 2013).

For example, in the Bighorn Basin, Wyoming, USA, where there has been extensive plant fossil research, flora shifted considerably during the PETM (McInerney and Wing, 2011; Wing and Currano, 2013). Plants that are typically adapted to intermediate moisture levels (particularly conifers) decreased, and thermophilic and dry-tolerant species (particularly Fabaceae (legumes)) surged in abundance (Wing and Currano, 2013). Hence, the western USA flora during the PETM was most similar to dry tropical forests.

Despite some regional variations, generally flora expanded toward higher latitudes, such as was observed in the Bighorn Basin (Wing and Currano, 2013). In the Arctic, pollen counts and biomarkers indicate that angiosperm abundance increased at the expense of gymnosperms (Schouten et al., 2007; Sluijs et al., 2006), while moisture transport increased, as suggested by changes in the δD of *n*-alkanes (Pagani et al., 2006).

Boucsein and Stein (2009) analyzed characteristics of organic particles, or macerals, in Arctic Ocean sediments (Integrated Ocean Drilling Program (IODP) site 302) from the late Cretaceous to the Eocene. Based on changes in the proportion of inertinite (regarded as an indicator of fire occurrence) relative to other terrigenous and aquatic macerals, the authors suggested that greater inputs of burned vegetation were deposited in the marine sediments during the Paleocene relative to the PETM and early Eocene.

Moore and Kurtz (2008) examined graphitic black carbon, a combustion byproduct, from two IODP sites: site 1210 (Shatsky Rise) and the Bass River section (New Jersey Margin). At Shatsky Rise, black carbon concentrations were below detection (<0.5 ppm), while at the New Jersey Margin, there was no clear pattern in black carbon flux at the onset or during the CIE. Carbon isotope analyses of black carbon revealed a ~3.5‰ negative CIE, which linked burned

material to PETM biomass, rather than burning of older Paleocene peat or coal (Moore and Kurtz, 2008).

Collinson et al. (2009) linked a shift in fire regime to changes in vegetation composition across the PETM in England. Late Paleocene samples, from the Cobham Lignite Bed in southern England, were dominated by charcoal associated with episodic fires and by fern spores, which suggested a low diversity, fire-prone community mainly composed of ferns and woody angiosperms. The PETM vegetation was characterized by a loss of ferns, an increase in wetland plants, and decreased fire occurrence. This study highlights the importance of vegetation (e.g., composition and fire-prone species) in determining fire propensity. Given the global geographic and compositional changes in PETM vegetation, which are often linked to precipitation and temperature patterns, predictions of fire occurrence are not easily extrapolated from changes in the quantity of biomass and aridity.

The concept of biomass and aridity as key fire drivers has its roots in fire history reconstructions of the past decades to 21,000 years, mainly derived from sedimentary charcoal and tree ring fire scar analyses. These reconstructions provide information regarding fire frequency, fire extent, and the timing of past fires in relation to climate (Daniau et al., 2012; Margolis and Balmat, 2009). The records reveal complexity and that multiple factors influence the relationship between fire occurrence and climate. But overall and in simplified terms, wet periods allow for the buildup of biomass (fuel) and dry periods facilitate the burning of vegetation (fuel availability). Increased precipitation can result in opposite effects on the susceptibility to fire depending on the initial wetness of the environment. In relatively wet environments that are likely not limited by fuel abundance, precipitation increases fuel moisture

and dampens fire occurrence; in dry environments that are fuel-limited, precipitation increases the amount of fuel and increases the ecosystems tendency toward fire (Daniau et al., 2012).

The length of wet and dry periods can also have different effects on fire occurrence depending on fuel type. Holocene fire frequency records in the western USA indicate that enhanced seasonality and anomalously wet years followed by anomalously dry years promoted fire conditions for vegetation with annual fuel production, such as grass (Margolis and Balmat, 2009). Other studies have suggested that extended dry periods led to widespread fires, such as the 1997 Indonesian fires that spread wildly during the long El Niño dry season, likely because heavier fuels (e.g., branches and logs) respond to humidity changes more slowly than finer fuels (e.g., grass and small twigs) (Page et al., 2002). Alternatively, during long-term droughts, fire occurrence can decrease if there is insufficient biomass to burn (Flannigan et al., 2009).

Changes in vegetation type can modify the link between climate and fire by affecting, for example, the abundance, structure, and moisture content of fuels (Higuera et al., 2014). In ecosystems with dense, continuous vegetation, fire occurrence is limited by climatic conditions that facilitate the drying of fuels. In contrast, in systems with low biomass abundance or discontinuous fuels, fire occurrence can be limited by the scarcity of burnable materials, even if climate conditions may have been conducive for fire (Higuera et al., 2014).

From the analysis of a global compilation of charcoal records covering the last 21,000 years, Daniau et al. (2012) found an overall increase in fire occurrence with increased temperature. Such findings tend to influence studies of ancient climate, and authors often postulate that hotter and drier conditions likely increased fire occurrence (Secord et al., 2010; Wing et al., 2005).

Pyrogenic carbon is a continuum of combustion products generated as solid residue or volatiles, ranging from slightly charred material to soot (Knicker, 2011; von Lützow et al., 2006). Polycyclic aromatic hydrocarbons (PAHs), which are part of this continuum, are byproducts of combustion released as volatiles and in association with particles. In the sedimentary record, changes in PAH concentrations are usually interpreted to indicate changes in fire occurrence, with more PAHs linked to increased fire occurrence (e.g., Marynowski and Simoneit, 2009; Denis et al., 2012). Aromatic structures tend to make pyrogenic carbon, including larger PAHs (≥5 rings), relatively resistant to degradation in soil environments and marine sediments (Knicker, 2011; von Lützow et al., 2006). For example, charcoal, another byproduct of fire, has a relatively long residence time in modern soils, estimated on the order of 500 – 10,000 years, and in marine sediments with oxygen exposure, 10,000 – 20,000 years (Knicker, 2011; von Lützow et al., 2006). Thus, in soils, larger fire-derived PAHs represent an intermediate-phase of refractory carbon that is relatively stable and less reactive than fresh biomass or litter, although they are not as refractory as fossil kerogens that may end up in paleosols from weathered parent lithologies (Denis, 2016). In marine sediments, however, PAHs likely reflect production (via combustion) to a greater extent than weathered inputs given the significantly better preservation of all carbon phases relative to soils (Freeman and Colarusso, 2001).

In this study, we analyzed PAHs and plant biomarkers in a sediment core from the central Arctic Ocean (IODP Hole 302-4A) in relation to biomass proxies for vegetation and precipitation in the Arctic before, during, and after the PETM. PAH and plant biomarker abundances provide a unique set of tools to evaluate to what extent the combination of hotter and wetter conditions (Pagani et al., 2006) and major changes in vegetation composition (Schouten et al., 2007; Sluijs

et al., 2006) impacted fire occurrence. If the ecosystem was not biomass-limited, then inferred wetter conditions would have dampened fire occurrence during the PETM in the Arctic. By evaluating changes in combustion (using PAHs) relative to terrestrial productivity (based on terpenoid biomarkers and pollen records), we seek insights into potential changes in biomass carbon in the Arctic region during a warm, wet, and high-CO_2 climate.

2. Study Section

Core samples were collected from IODP Hole 302-4A on the Lomonosov Ridge in the central Arctic Ocean (Figure 1). Several previous studies have analyzed these samples, or samples from similar stratigraphic intervals, for a variety of geochemical, biomarker, and palynomorph data (Backman et al., 2006; Boucsein and Stein, 2009; Knies et al., 2008; Pagani et al., 2006; Schouten et al., 2007; Sluijs et al., 2008b, 2006; Stein, 2008; Stein et al., 2014, 2006; Weller and Stein, 2008). The organic-rich siliciclastic claystone sediments contain well-preserved biomarkers and palynomorphs (Pagani et al., 2006; Schouten et al., 2007; Sluijs et al., 2006; Stein et al., 2006; Weller and Stein, 2008) before, during, and after the PETM interval. Anoxic bottom-water conditions (interpreted based on the presence of laminated sediments, the absence of benthic foraminiferal linings, C/S ratios, and biomarkers) and euxinic conditions in the photic zone (interpreted based on the presence of isorenieratene and other isorenieratene derivatives) facilitated organic carbon preservation during the PETM interval (Schouten et al., 2007; Sluijs et al., 2006; Stein et al., 2006; Weller and Stein, 2008). Average sedimentation rates from the late Paleocene to the early Eocene were 1 to 3 cm/kyr (Sluijs et al., 2008b; Stein et al., 2006) and were estimated to have increased during the PETM to 5.0 ± 1.2 cm/kyr (Sluijs et al., 2008b). Sea level rose during the event by approximately 20 to 30 m (Sluijs et al., 2008a).

The Arctic region was hotter and wetter during the PETM than before and after the event (Pagani et al., 2006; Sluijs et al., 2008b, 2006). Air temperatures increased 6°C during the PETM from ~15°C to ~21°C (Peterse et al., 2012; Weijers et al., 2007). Pagani et al. (2006) suggested a greater export of moisture from the tropics towards higher latitudes. The isotopic composition of Arctic PETM precipitation was considerably ^{2}H-enriched compared to today, indicating reduced rainout along the source airmass' trajectory from lower latitudes to the poles. In addition, low-salinity-tolerant dinocyst assemblages (Sluijs et al., 2006) suggest increased precipitation and runoff during the PETM (Pagani et al., 2006). Sluijs et al. (2006) suggested that higher temperatures and enhanced fluvial runoff increased nutrient inputs, which increased marine productivity, and caused water column stratification. Furthermore, because the Arctic Basin may have been a restricted basin, high terrestrial runoff during the PETM could have helped create a freshwater upper layer that resulted in water column stratification (Sluijs et al., 2006).

3. Methods

3.1. Samples

Sediments were obtained from IODP Expedition 302 Hole 4A on the Lomonosov Ridge (Backman et al., 2006; Pagani et al., 2006) (Figure 1). An age model for the core was previously determined from palynological data and index events, which put the base of the Eocene at the top of Core 32x (Backman et al., 2006) (Figure 2 and Figure 3). The PETM interval was marked based on the negative carbon isotope excursion from δ^{13}C of total organic carbon and of leaf-wax *n*-alkanes (Pagani et al., 2006; Schouten et al., 2007).

3.2. Extraction and analysis

206 Lipid extracts analyzed in this paper were a subset of those processed and analyzed in
207 Pagani et al. (2006). Sediments were prepared for analysis as described in Pagani et al. (2006).
208 Briefly, sediments were freeze-dried and extracted with dichloromethane (DCM) using
209 accelerated solvent extraction. Total lipid extracts (TLEs) were separated by column
210 chromatography into three fractions using hexane (S1), hexane/DCM (9:1 *v:v*) (S2), and
211 DCM/methanol (2:1 *v:v*) (S3). The first fraction (S1) was further separated into two fractions
212 (adducts and non-adducts) via urea adduction.
213 PAHs and terpenoids were analyzed using an Agilent 6890 GC with an Agilent 5973
214 quadrupole mass spectrometer (MS) and a fused silica capillary column (Agilent J&W DB-5; 30
215 m, 250 μm, 0.25 μm). The column flow rate was 2.0 ml/min and the oven program started at
216 60°C for 1 min, ramped to 320°C at 6°C/min, and had a final hold time of 15 min. The MS had
217 an ionization energy of 70 eV with a scanning mass range of *m/z* 40-700 in Full Scan mode.
218 PAHs were identified and quantified in Full Scan mode based on authentic standards, NIST 98
219 spectral library, fragmentation patterns, and retention times. For quantification, extracted ions
220 were (*m/z*): 202 (pyrene), 237 (simonellite), 252 (simonellite, benzo[a]pyrene,
221 benzofluoranthene, perylene, 1,2,3,4-tetrahydro-2,2,9-trimethylpicene (i.e., "β-amyrin
222 derivative", referred to as "tetra-aromatic triterpane" in Schouten et al. (2007)), 255
223 (dehydroabietane), 268 (β-amyrin derivative), 300 (coronene), 324 (β-amyrin derivative), 367
224 (hope-(17,21)-ene). *n*-Alkanes were from S1 Adducts (*m/z*): 43 and 57; pristane and phytane
225 were from S1 Non-adducts (*m/z*): 57. Relative abundances were determined based on relative
226 peak areas of compounds within a given fraction.
227
228 *3.3. Normalized plant biomarker abundance to terrestrial organic carbon inputs*

To account for production and preservation changes in TOC and eliminate the influence of changing marine organic carbon (TOC_{marine}) inputs, we normalized plant biomarker abundances (Schouten et al., 2007) to terrestrial organic carbon (TOC_{terr}) (Figure 3) rather than TOC (TOC_{marine} + TOC_{terr}). We used two proxies for terrestrial and marine biomass contributions (Sluijs and Dickens, 2012) to estimate the relative proportions of TOC_{terr} and TOC_{marine}, the BIT index and the relative portions of terrestrial (pollen and spores) and marine (primarily dinoflagellate cysts) palynomorphs. The BIT index is based on the proportion of specific ether lipids (glycerol dialkyl glycerol tetraethers (GDGTs)) as defined by Hopmans et al. (2004). Distinctive terrestrial GDGTs are produced by bacteria in soils and rivers, while the marine GDGT is primarily produced by pelagic archaea in the ocean. To calculate TOC_{terr}, for each sample we multiplied the TOC value by the percentage of terrestrial inputs based on palynomorphs or the BIT index based on values reported by Sluijs et al. (2006). Because both proxies have limitations (Sluijs and Dickens, 2012), we used the average of the TOC_{terr} calculated by the two proxies. Uncertainty was the difference between TOC_{terr} calculated from the proxies individually for a given sample (Figure 2 and Figure S1).

4. Results

PAH abundance increased relative to both diterpenoid and triterpenoid abundances in PETM sediments compared to late Paleocene sediments (Figure 2). Coronene/coronene+pyrene ratios across the section were an average of 0.3 and ranged from 0.1 to 0.7 (Figure S1).

The ratio of the sum of odd *n*-C_{25} to *n*-C_{33} alkanes relative to diterpenoids (simonellite and dehydroabietane derived from gymnosperms) was similar to pollen composition trends and significantly greater than the ratio of β-amyrin derivative relative to diterpenoids (based on *n*-

252 alkanes, pollen, and terpenoid data from Schouten et al. (2007)) (Figure 2). The percent of the
253 sum of the *n*-alkanes ratio ranged from 46% to 58% in the late Paleocene, 55% to 88% in the
254 PETM, and 52% to 77% in the early Eocene. Air temperature and percent of angiosperms
255 (pollen) in the PETM and post-PETM section are linearly correlated ($R^2 = 0.68$), but not as well
256 correlated across the section ($R^2 = 0.33$) (Figure S2) (based on temperature data from Peterse et
257 al. (2012)).

258 Pristane/phytane ratios (Pr/Ph) (Figure 2) were generally lower in PETM sediments than
259 before or after the event and ranged from 0.1 to 3.1 throughout the whole sampled section. Pr/Ph
260 ratios in Paleocene pre-PETM sediments ranged from 0.1 to 1.6. Ratios for PETM interval
261 sediments were less than 1 for most of the PETM, except for elevated values at ~382.5 mcd.
262 Ratios for Eocene post-PETM sediments ranged from 0.3 to 3.1, with Eocene Pr/Ph ratios less
263 than 1 immediately after the PETM interval, and then greater than 1 at 379 to 378 mcd.

264 Concentrations (ng/g TOC_{terr}) of dehydroabietane, simonellite, β-amyrin derivative, and
265 $C_{25\text{-}33}$ *n*-alkanes had little variation across the PETM event (though they were more variable
266 before and after the event) except for a peak in biomarker and angiosperm pollen abundance at
267 the end of the CIE (Figure 3).

268

269 **5. Discussion**

270 *5.1. Relationship between PAHs and plant biomarkers*

271 PAH concentrations increased relative to plant aromatic biomarkers in PETM sediments
272 compared to pre-PETM sediments (Figure 2). Differential preservation, transportation, or
273 production could explain the observed increase in PAH abundance, but changes in PAH
274 production was more likely for several reasons.

Transportation differences cannot fully explain the observed increase in the abundance of PAHs relative to plant biomarkers because the transport mechanisms of both compounds by air and water are similar (Baek et al., 1991). Both PAHs and aromatic plant biomarkers have similar chemical structures with multiple aromatic rings and would likely have similar preservation potential (Sluijs et al., 2006). Each class has compounds that cover a range of sizes; for example, PAHs analyzed here range from 202 g/mol to 300 g/mol, while simonellite has a mass of 252 g/mol and 1,2,3,4-tetrahydro-2,2,9-trimethylpicene (i.e., "β-amyrin derivative", referred to as "tetra-aromatic triterpane" in Schouten et al. (2007)) has a mass of 324 g/mol.

Favorable conditions for organic carbon preservation before, during, and after the PETM (Pagani et al., 2006; Schouten et al., 2007; Sluijs et al., 2006; Stein et al., 2006; Weller and Stein, 2008) are further supported by the dominance of pyrene (4-ring PAH) over coronene (7-ring PAH) throughout the section (Figure S1). Lower molecular weight PAHs are more susceptible to degradation than higher molecular weight PAHs because of their greater solubility and bioavailability (May et al., 1978). The coronene/coronene+pyrene ratio averaged 30% and had no trend across the section. The dominance of pyrene in the Arctic marine sediments contrasts starkly with the dominance of larger PAHs like coronene in highly degraded PETM terrestrial paleosols (Denis, 2016). Therefore, the ratio of PAHs to plant biomarkers should not have been altered due to lack of preservation. We conclude that PAH abundances primarily reflect changes in PAH production and, thus, general trends in fire occurrence.

5.2. Percent of angiosperms relative to gymnosperms based on plant biomarkers and pollen

Schouten et al. (2007) observed that plant biomarker (triterpenoid/diterpenoid) ratios underestimated plant type composition (angiosperms versus gymnosperms) compared to

298 estimates using pollen, and the authors suggested that taphonomic differences accounted for the
299 observed discrepancies in the percentage of angiosperms relative to gymnosperms. Based on
300 more recent literature, triterpenoids (derived from angiosperms), such as β-amyrin derivative, are
301 not preserved as well as diterpenoids (derived from gymnosperms) in terrestrial sediments
302 (Diefendorf et al., 2014). Triterpenoid-to-diterpenoid ratios, therefore, underestimate the
303 abundance of angiosperms in the source paleovegetation, which accounts for the discrepancy
304 between biomarker and pollen indicators of angiosperms reported by Schouten et al. (2007).
305 Following the suggested practice of Diefendorf et al. (2014), we used the ratio of plant wax *n*-
306 alkanes to diterpenoids as a proxy for the relative abundance of angiosperms to gymnosperms in
307 paleovegetation.

308 Across the PETM section, the concentration profile of the C_{29} *n*-alkane is similar to the
309 angiosperm pollen abundance profile and is dissimilar to that of the terrestrial plant aromatic
310 biomarkers (Figure 3). Although many angiosperms and gymnosperms produce *n*-alkanes, the
311 conifer families that do are primarily common today in Asia and the Southern Hemisphere (e.g.,
312 Podocarpaceae (Diefendorf et al., 2015)). It is unlikely that these conifers lived in the Arctic
313 during the PETM (Basinger et al., 1994). Aside from Podocarpaceae, the major conifer groups
314 produce hardly any C_{29} *n*-alkane; therefore, the C_{29} *n*-alkane provides a strong phylogenetic
315 signal for angiosperm inputs (Diefendorf et al., 2015). The paleovegetation proxy introduced by
316 Diefendorf et al. (2014), which quantifies the ratio of *n*-alkanes to diterpenoids, yields estimates
317 of angiosperm inputs that match the pollen record (Figure 2). These findings are consistent with
318 the work by Diefendorf et al. (2014) on terpenoid preservational biases. Both the *n*-alkanes-to-
319 diterpenoids ratios and pollen data indicate that the relative contribution of angiosperms

increased during the PETM from ~55% to ~80%, reflecting a significant ecological shift to angiosperm-dominated vegetation.

5.3. Terrestrial plant inputs

Organic geochemical studies typically normalize biomarker abundances to total organic carbon (TOC) in order to account for changes in organic carbon production and preservation. However, in these sediments there are two sources of carbon, marine-derived (TOC_{marine}) and terrestrially derived (TOC_{terr}). Because TOC_{marine} can vary independently from terrestrial organic contributions (Sluijs et al., 2006; Stein et al., 2006), normalizing the abundance of plant-derived compounds to TOC_{terr}, will better represent landscape signals. A variety of evidence indicates that the relative proportions of TOC_{terr} and TOC_{marine} changed before, during, and after the PETM.

Evidence from palynomorphs (dinoflagellate cysts, pollen, and spores), the Branched and Isoprenoid Tetraether (BIT) index (Hopmans et al., 2004), biomarkers (e.g., high amounts of long-chain *n*-alkanes and long-chain *n*-fatty acids), and the Rock Eval hydrogen index suggested that the uppermost Paleocene sediments were proximal to the coast and were more terrestrially influenced by riverine inputs (Sluijs et al., 2006; Stein et al., 2006; Weller and Stein, 2008). During the PETM interval, evidence indicates that aquatic carbon dominated inputs (Sluijs et al., 2006; Stein et al., 2006; Weller and Stein, 2008). Pr/Ph ratios are consistent with these interpretations (Figure 2). Pr/Ph ratios <1 indicate marine inputs and ratios >1 indicate increasing dominance of terrestrial inputs (typically >3) (Peters et al., 2005). At the end of the PETM, Pr/Ph ratios >1 coincide with low and non-detectable amounts of isorenieratene and monoaromatic isorenieratene derivatives, which signify a return to an oxic photic zone and oxic depositional

conditions. Overall, multiple lines of evidence indicate that elevated marine sourced organic inputs were preserved during the CIE interval (Knies et al., 2008; Sluijs et al., 2006; Stein, 2008; Stein et al., 2006; Weller and Stein, 2008; Figure 2). Although there is evidence for increased terrestrial runoff during the CIE elsewhere (e.g., Crouch et al., 2003), a rise in sea level during the PETM likely reduced the amount of terrestrial material that reached the Lomonosov Ridge (Sluijs et al., 2008a). In addition, increased marine productivity (Knies et al., 2008; Sluijs et al., 2008b; Stein, 2008; Stein et al., 2014) likely further diluted the relative proportion of TOC_{terr} preserved in the PETM sediments.

Normalized concentrations (ng/g TOC_{terr}) of dehydroabietane, simonellite, β-amyrin derivative, and $C_{25\text{-}33}$ *n*-alkanes, provide a means of investigating a general pattern of biomarker input (without getting quantitative accumulation numbers) across the PETM. Biomarker data show that plant input did not change drastically across the PETM event (Figure 3). As previously noted, biomarkers and pollen data indicate greater inputs from angiosperms during the PETM, and both biomarker (*n*-alkanes/diterpenoids) and pollen indicators show similar trends for most of the record, although they diverged at the end of the PETM. The discrepancy occurs from 382.4 to 381.4 mcd as $\delta^{13}C_{org}$ values and temperatures recovered to pre-PETM values and when isorenieratene and monoaromatic isorenieratene derivatives were below detection limit in the samples, which signified a return to an oxic photic zone (Figure 2 and Figure 3).

5.4. Fire and ecosystem change implications

Changes in angiosperm inputs correlate with proxy evidence for warming air temperatures based on the Methylation of Branched Tetraether (MBT) and the Cyclisation of Branched Tetratether (CBT) indices (Weijers et al., 2007; Peterse et al., 2012; Figure S2) and

366 followed an inferred increase in moisture to the Arctic (Pagani et al., 2006). As temperature
367 increased, angiosperm pollen increased at the expense of both gymnosperm pollen and fern
368 spores, and then angiosperm pollen decreased at the end of the PETM, as the climate cooled. The
369 trend of increased angiosperms and decreased gymnosperms was observed elsewhere during the
370 PETM, including Spitsbergen, the North Sea, Spain, and New Zealand (Wing and Currano,
371 2013, and references therein). Sluijs et al. (2006) suggested that the increased abundance of
372 angiosperm vegetation (Figure S3) in the Arctic reflected an expanded growing season. Based on
373 the taxonomy of the pollen from the Arctic sediments, during the body of the CIE the vegetative
374 landscape may have been an angiosperm-dominated temperate forest, which included some
375 tropical plants (such as palms) (D. Willard, pers. comm. 2016). During the CIE recovery, as
376 environmental conditions started to recover to pre-PETM conditions, angiosperms decreased and
377 gymnosperms and ferns increased giving way to an ecosystem with more swampy or wetland
378 plants (D. Willard, pers. comm. 2016).

379 We interpret PAH abundances relative to aromatic plant biomarkers to reflect changes in
380 PAH production. The rise in normalized PAH values suggests that increased fire occurrence was
381 associated with the angiosperm vegetation shift, perhaps indicating greater prevalence of more
382 fire-prone or fire-adapted species, as was observed in England (Collinson et al., 2009), greater
383 biomass abundance, or increased continuity of fuels that enhanced the ability for fire to spread.
384 Based on empirical fire models of the modern in the United States, doubling of atmospheric CO_2
385 increased the frequency of lightning strikes and increased fire occurrence by nearly 50%, which
386 suggests that the CO_2-rich atmosphere during the PETM may have increased lightning strike
387 frequency and enhanced fire occurrence in the Arctic (Price and Rind, 1994).

The increased moisture transport to the Arctic (Pagani et al., 2006) preceded the coincident increases in temperature, angiosperms, and PAHs (Figure 2). The time lag emphasizes that a combination of factors influenced changes in fire occurrence, including a balance of fuel composition (e.g., vegetation amount and type), fuel availability (e.g., amount of vegetation that can burn based on humidity, precipitation, and temperature), and ignition sources (e.g., lightning).

The high-latitude position of the Arctic means that the Paleocene-Eocene ecosystems functioned under strong light seasonality (continuous winter darkness, continuous summer light) and short transitional seasons (e.g., lasting less than 60 days). Despite these extreme natural light conditions, a diverse forest ecosystem can survive, such has been observed from fossil evidence in terrestrial sediments deposited in the early to mid-Eocene, a different time period but still a warm and humid climate (Jahren and Sternberg, 2003). The terrestrial mean annual temperature (MAT) for the Arctic in the early Eocene was 13.2 ± 2.0°C, as estimated from oxygen-isotope equilibration between environmental water and pedogenic carbonate from Axel Heiberg Island (Jahren and Sternberg, 2003; Figure 1). In addition, cold-month temperatures were above 0°C, which implies a lack of freeze events (Basinger et al., 1994; Jahren and Sternberg, 2003). The estimated terrestrial MAT for the late Paleocene was ~15°C and increased to ~21°C during the PETM based on the distribution of branched glycerol dialkyl glycerol tetraether (GDGT) membrane lipids (the MBT-CBT proxy) (Peterse et al., 2012; Weijers et al., 2007). Similar to Axel Heiberg Island in the early Eocene, the continental Arctic during the PETM likely had cold-month temperatures above freezing.

The warmer temperatures and wetter conditions during the PETM may have stymied gymnosperm growth and, by reducing competition, opened up the ecosystem to angiosperms.

411 Alternatively, angiosperms may have migrated, with rising temperatures, from lower latitudes.
412 The angiosperm community may have recovered more rapidly after fire disturbances than
413 gymnosperms, potentially due to higher productivity or higher reproductive rates (Bond and
414 Midgley, 2012). As temperatures cooled at the end of the PETM, gymnosperm populations were
415 revived, and the ecosystem shifted back to a less fire-prone community. A potential scenario is
416 that fire increased in an angiosperm-dominated temperate forest, which included some tropical
417 plants (e.g., palms), and then as pre-PETM conditions began to return, gymnosperms and ferns
418 recovered, angiosperms decreased, and there was a greater abundance of swampy or wetland
419 plants (D. Willard, pers. comm. 2016), which were not as conducive to fire.
420 Based on our study and the few other studies of fire occurrence during the PETM,
421 changes in fire occurrence varied by location. At IODP site 1210 (Shatsky Rise) in the west-
422 central Pacific, there was no evidence of fire occurrence; at the New Jersey margin (Bass River
423 section) there was evidence of fire, but no clear change in occurrence during the PETM (Moore
424 and Kurtz, 2008). In England, fire occurrence decreased and was associated with a change in
425 vegetation; in this case, a shift from an herbaceous fern and woody angiosperm fire-prone system
426 to less ferns and woody plants, and increased wetland plants (Collinson et al., 2009). Although
427 during the PETM fire occurrence decreased in England but increased in the Arctic, in both
428 records, increased fire occurrence corresponded to an angiosperm-dominated community and
429 decreased fire occurrence was associated with increased wetland plants. Overall, the variability
430 in the effect of global warming on fire occurrence likely reflects local or regional variations in
431 ecosystems (e.g., vegetation type, structure, and amount) and environmental conditions (e.g.,
432 precipitation).
433

5.5. Carbon cycle implications

Plant CO_2-enrichment studies (Bowes, 1993) suggest that plant biomass may have increased during the high CO_2 conditions of the PETM. In these studies, plants accumulated 30% more biomass when atmospheric CO_2 was doubled (pCO_2 was increased from ~350 ppm to ~650 ppm) (Bowes, 1993). Angiosperms tend to have higher maximum growth rates than gymnosperms (Bond, 1989), thus increased angiosperm production during the PETM is consistent with higher terrestrial productivity. Increased terrestrial plant productivity had potential to help sequester CO_2 from the atmosphere through greater accumulation of biomass in soils or coastal marine sediments, both of which can serve as a sink for carbon. Yet, despite the potential for greater terrestrial organic matter burial, the site 302 record shows a relatively constant pattern of $\%TOC_{terr}$ before and during the PETM event. In contrast, $\%TOC_{marine}$ increased significantly during the PETM, which is consistent with increased marine productivity and greater marine organic matter burial (Knies et al., 2008; Sluijs et al., 2006; Stein, 2008; Stein et al., 2014). While there likely was increased terrestrial productivity in the warmer and wetter Arctic region, our PAH record indicates that it is possible that fire occurrence was a major factor that reduced the transfer of terrestrial plant carbon to soil and sedimentary carbon. Because plant biomass burning adds CO_2 to the atmosphere, greater fire occurrence may have prevented a significant sequestration of carbon by terrestrial plant photosynthesis.

6. Conclusions

In the Arctic during the PETM, the landscape shifted to an angiosperm-dominated ecosystem, but terrestrial plant input into the marine realm remained nearly constant. Similar to observations by Diefendorf et al. (2014), the triterpenoid to diterpenoid ratio for the composition

of angiosperms relative to gymnosperms underestimated the percentage of angiosperms. Instead, a ratio of *n*-alkanes to diterpenoids was similar to the angiosperm composition observed in pollen.

During the PETM, PAH abundance increased relative to plant biomarkers compared to before or after the event. Wetter conditions followed by higher temperatures favored angiosperms, and this compositional shift in vegetation was associated with enhanced fire occurrence. Hence, in paleoenvironments, increased fire occurrence was not always directly linked to drier conditions. In the Arctic during the PETM, a climate-driven shift to an angiosperm-dominated plant community spurred greater fire occurrence. Greater biomass burning may have attenuated the effects of increases in plant productivity on the carbon cycle, and thus potentially hindered any significant changes in terrestrial organic carbon sequestration.

Acknowledgements

We thank the Integrated Ocean Drilling Program (IODP) Expedition 302 Scientists. For instrument assistance, Denny Walizer (Pennsylvania State University) and Irene Rijpstra (NIOZ). For insightful discussions, Lee Kump, Liz Hajek, Margot Kaye, and Deb Willard. For help with editing, Amy Goldman. Two anonymous reviewers are thanked for their helpful comments. EHD was supported by the National Science Foundation (NSF) Graduate Research Fellowship under Grant No. DGE1255832, American Geological Institute (AGI) Harriet Evelyn Wallace Scholarship, and funding from the Pennsylvania State University's Paul D. Krynine Scholarship, ConocoPhillips Graduate Student Fellowship, and Hiroshi and Koya Ohmoto Graduate Fellowship; SS was supported by the Netherlands Earth System Science Centre

(NESSC), financially supported by the Ministry of Education, Culture and Science (OCW).

References

Backman, J., Moran, K., MicInroy, D.B., Mayer, L.A., the Expedition 302 Scientists, 2006. Sites M0001–M0004, in: Proceedings of the Integrated Ocean Drilling Program, 302. Integrated Ocean Drilling Program Management International, Inc., Edinburgh. doi:10.2204/iodp.proc.302.104.2006

Baek, S.O., Field, R.A., Goldstone, M.E., Kirk, P.W., Lester, J.N., Perry, R., 1991. A review of atmospheric polycyclic aromatic hydrocarbons: Sources, fate and behavior. Water. Air. Soil Pollut. 60, 279–300. doi:10.1007/BF00282628

Basinger, J.F., Greenwood, D.R., Sweda, T., 1994. Early Tertiary vegetation of Arctic Canada and its relevance to paleoclimatic interpretation, in: Boulter, M.C. (Ed.), Arctic Plants and Climates: 65 Million Years of Change. Springer-Verlag, Berlin.

Bond, W.J., 1989. The tortoise and the hare: ecology of angiosperm dominance and gymnosperm persistence. Biol. J. Linn. Soc. 36, 227–249. doi:10.1111/j.1095-8312.1989.tb00492.x

Bond, W.J., Midgley, J.J., 2012. Fire and the angiosperm revolutions. Int. J. Plant Sci. 173, 569–583. doi:10.1086/665819

Boucsein, B., Stein, R., 2009. Black shale formation in the late Paleocene/early Eocene Arctic Ocean and paleoenvironmental conditions: New results from a detailed organic petrological study. Mar. Pet. Geol. 26, 416–426. doi:10.1016/j.marpetgeo.2008.04.001

Bowes, G., 1993. Facing the inevitable: Plants and increasing atmospheric CO2. Annu. Rev. Plant Physiol. Plant Mol. Biol. 44, 309–332.

Collinson, M.E., Steart, D.C., Harrington, G.J., Hooker, J.J., Scott, A.C., Allen, L.O., Glasspool, I.J., Gibbons, S.J., 2009. Palynological evidence of vegetation dynamics in response to palaeoenvironmental change across the onset of the Paleocene-Eocene Thermal Maximum at Cobham, Southern England. Grana 48, 38–66. doi:10.1080/00173130802707980

Crouch, E.M., Dickens, G.R., Brinkhuis, H., Aubry, M.P., Hollis, C.J., Rogers, K.M., Visscher, H., 2003. The Apectodinium acme and terrestrial discharge during the Paleocene-Eocene thermal maximum: New palynological, geochemical and calcareous nannoplankton observations at Tawanui, New Zealand. Palaeogeogr. Palaeoclimatol. Palaeoecol. 194, 387–403. doi:10.1016/S0031-0182(03)00334-1

Cui, Y., Kump, L.R., Ridgwell, A.J., Charles, A.J., Junium, C.K., Diefendorf, A.F., Freeman, K.H., Urban, N.M., Harding, I.C., 2011. Slow release of fossil carbon during the Palaeocene–Eocene Thermal Maximum. Nat. Geosci. 4, 481–485. doi:10.1038/ngeo1179

Daniau, A.L., Bartlein, P.J., Harrison, S.P., Prentice, I.C., Brewer, S., Friedlingstein, P., Harrison-Prentice, T.I., Inoue, J., Izumi, K., Marlon, J.R., Mooney, S., Power, M.J., Stevenson, J., Tinner, W., Andrič, M., Atanassova, J., Behling, H., Black, M., Blarquez, O., Brown, K.J., Carcaillet, C., Colhoun, E.A., Colombaroli, D., Davis, B.A.S., D'Costa, D., Dodson, J., Dupont, L., Eshetu, Z., Gavin, D.G., Genries, A., Haberle, S., Hallett, D.J., Hope, G., Horn, S.P., Kassa, T.G., Katamura, F., Kennedy, L.M., Kershaw, P., Krivonogov, S., Long, C., Magri, D., Marinova, E., McKenzie, G.M., Moreno, P.I., Moss, P., Neumann, F.H., Norstrm, E., Paitre, C., Rius, D., Roberts, N., Robinson, G.S., Sasaki, N., Scott, L., Takahara, H., Terwilliger, V., Thevenon, F., Turner, R., Valsecchi, V.G., Vannière, B.,

Walsh, M., Williams, N., Zhang, Y., 2012. Predictability of biomass burning in response to climate changes. Global Biogeochem. Cycles 26, 1–12. doi:10.1029/2011GB004249
Denis, E.H., 2016. Production and preservation of organic and fire-derived carbon across the Paleocene-Eocene Thermal Maximum. The Pennsylvania State University.
Denis, E.H., Toney, J.L., Tarozo, R., Anderson, R.S., Roach, L.D., Huang, Y., 2012. Polycyclic aromatic hydrocarbons (PAHs) in lake sediments record historic fire events: Validation using HPLC-fluorescence detection. Org. Geochem. 45, 7–17. doi:10.1016/j.orggeochem.2012.01.005
Diefendorf, A.F., Freeman, K.H., Wing, S.L., 2014. A comparison of terpenoid and leaf fossil vegetation proxies in Paleocene and Eocene Bighorn Basin sediments. Org. Geochem. 71, 30–42. doi:10.1016/j.orggeochem.2014.04.004
Diefendorf, A.F., Leslie, A.B., Wing, S.L., 2015. Leaf wax composition and carbon isotopes vary among major conifer groups. Geochim. Cosmochim. Acta 170, 145–156. doi:10.1016/j.gca.2015.08.018
Flannigan, M.D., Krawchuk, M.A., De Groot, W.J., Wotton, B.M., Gowman, L.M., 2009. Implications of changing climate for global wildland fire. Int. J. Wildl. Fire 18, 483–507. doi:10.1071/WF08187
Freeman, K.H., Colarusso, L.A., 2001. Molecular and isotopic records of C4 grassland expansion in the late Miocene. Geochim. Cosmochim. Acta 65, 1439–1454. doi:10.1016/S0016-7037(00)00573-1
Hessl, A.E., 2011. Pathways for climate change effects on fire: Models, data, and uncertainties. Prog. Phys. Geogr. 35, 393–407. doi:10.1177/0309133311407654
Higuera, P.E., Brubaker, L.B., Anderson, P.M., Hu, F.S., Brown, T.A., 2014. Vegetation mediated the impacts of postglacial climate change on fire regimes in the south-central Brooks Range , Alaska 79, 201–219. doi:10.1890/07-2019.1
Hopmans, E.C., Weijers, J.W.H., Schefuß, E., Herfort, L., Sinninghe Damsté, J.S., Schouten, S., 2004. A novel proxy for terrestrial organic matter in sediments based on branched and isoprenoid tetraether lipids. Earth Planet. Sci. Lett. 224, 107–116. doi:10.1016/j.epsl.2004.05.012
Jahren, A.H., Sternberg, L.S.L., 2003. Humidity estimate for the middle Eocene Arctic rain forest. Geology 31, 463–466. doi:10.1130/0091-7613(2003)031<0463:HEFTME>2.0.CO;2
Knicker, H., 2011. Pyrogenic organic matter in soil: Its origin and occurrence, its chemistry and survival in soil environments. Quat. Int. 243, 251–263. doi:10.1016/j.quaint.2011.02.037
Knies, J., Mann, U., Popp, B.N., Stein, R., Brumsack, H.J., 2008. Surface water productivity and paleoceanographic implications in the Cenozoic Arctic Ocean. Paleoceanography 23, 1–12. doi:10.1029/2007PA001455
Kraus, M.J., Riggins, S., 2007. Transient drying during the Paleocene-Eocene Thermal Maximum (PETM): Analysis of paleosols in the Bighorn Basin, Wyoming. Palaeogeogr. Palaeoclimatol. Palaeoecol. 245, 444–461. doi:10.1016/j.palaeo.2006.09.011
Margolis, E.Q., Balmat, J., 2009. Fire history and fire-climate relationships along a fire regime gradient in the Santa Fe Municipal Watershed, NM, USA. For. Ecol. Manage. 258, 2416–2430. doi:10.1016/j.foreco.2009.08.019
Marynowski, L., Simoneit, B.R.T., 2009. Widespread Upper Triassic to Lower Jurassic Wildfire records From Poland: Evidence From charcoal and pyrolytic polycyclic aromatic hydrocarbons. Palaios 24, 785–798. doi:10.2110/palo.2009.p09-044r
May, W.E., Wasik, S.P., Freeman, D.H., 1978. Determination of the solubility behavior of some

569 polycyclic aromatic hydrocarbons in water. Anal. Chem. 50, 997–1000.
570 doi:10.1021/ac50029a042
571 McInerney, F.A., Wing, S.L., 2011. The Paleocene-Eocene Thermal Maximum: A perturbation
572 of carbon cycle, climate, and biosphere with implications for the future. Annu. Rev. Earth
573 Planet. Sci. 39, 489–516. doi:10.1146/annurev-earth-040610-133431
574 Moore, E.A., Kurtz, A.C., 2008. Black carbon in Paleocene-Eocene boundary sediments: A test
575 of biomass combustion as the PETM trigger. Palaeogeogr. Palaeoclimatol. Palaeoecol. 267,
576 147–152. doi:10.1016/j.palaeo.2008.06.010
577 Pagani, M., Pedentchouk, N., Huber, M., Sluijs, A., Schouten, S., Brinkhuis, H., Sinninghe
578 Damsté, J.S., Dickens, G.R., 2006. Arctic hydrology during global warming at the
579 Palaeocene/Eocene thermal maximum. Nature 442, 671–675. doi:10.1038/nature05043
580 Page, S.E., Siegert, F., Rieley, J.O., Boehm, H.-D. V., Jaya, A., Limin, S., 2002. The amount of
581 carbon released from peat and forest fires in Indonesia during 1997. Nature 420, 61–66.
582 doi:10.1038/nature01141.1.
583 Peters, K.E., Walters, C.C., Moldowan, J.M., 2005. The Biomarker Guide. Volume 2:
584 Biomarkers and Isotopes in Petroleum Exploration and Earth History, 2nd ed. Cambridge
585 University Press, Cambridge.
586 Peterse, F., van der Meer, J., Schouten, S., Weijers, J.W.H., Fierer, N., Jackson, R.B., Kim, J.H.,
587 Sinninghe Damsté, J.S., 2012. Revised calibration of the MBT-CBT paleotemperature
588 proxy based on branched tetraether membrane lipids in surface soils. Geochim. Cosmochim.
589 Acta 96, 215–229. doi:10.1016/j.gca.2012.08.011
590 Price, C., Rind, D., 1994. The impact of a 2-X-Co2 climate on lightning-caused fires. J. Clim.
591 doi:10.1175/1520-0442(1994)007<1484:TIOACC>2.0.CO;2
592 Schouten, S., Woltering, M., Rijpstra, W.I.C., Sluijs, A., Brinkhuis, H., Sinninghe Damsté, J.S.,
593 2007. The Paleocene-Eocene carbon isotope excursion in higher plant organic matter:
594 Differential fractionation of angiosperms and conifers in the Arctic. Earth Planet. Sci. Lett.
595 258, 581–592. doi:10.1016/j.epsl.2007.04.024
596 Secord, R., Gingerich, P.D., Lohmann, K.C., Macleod, K.G., 2010. Continental warming
597 preceding the Palaeocene-Eocene thermal maximum. Nature 467, 955–958.
598 doi:10.1038/nature09441
599 Sluijs, A., Brinkhuis, H., Crouch, E.M., John, C.M., Handley, L., Munsterman, D., Bohaty, S.M.,
600 Zachos, J.C., Reichart, G.J., Schouten, S., Pancost, R.D., Sinninghe Damsté, J.S., Welters,
601 N.L.D., Lotter, A.F., Dickens, G.R., 2008a. Eustatic variations during the Paleocene-Eocene
602 greenhouse world. Paleoceanography 23, 1–18. doi:10.1029/2008PA001615
603 Sluijs, A., Dickens, G.R., 2012. Assessing offsets between the δ13C of sedimentary components
604 and the global exogenic carbon pool across early Paleogene carbon cycle perturbations.
605 Global Biogeochem. Cycles 26, 1–14. doi:10.1029/2011GB004224
606 Sluijs, A., Röhl, U., Schouten, S., Brumsack, H.J., Sangiorgi, F., Sinninghe Damsté, J.S.,
607 Brinkhuis, H., 2008b. Arctic late Paleocene-Early Eocene paleoenvironments with special
608 emphasis on the Paleocene-Eocene thermal maximum (Lomonosov Ridge, Integrated Ocean
609 Drilling Program Expedition 302). Paleoceanography 23, 1–17.
610 doi:10.1029/2007PA001495
611 Sluijs, A., Schouten, S., Pagani, M., Woltering, M., Brinkhuis, H., Sinninghe Damsté, J.S.,
612 Dickens, G.R., Huber, M., Reichart, G.-J., Stein, R., Matthiessen, J., Lourens, L.J.,
613 Pedentchouk, N., Backman, J., Moran, K., the Expedition, S., 2006. Subtropical Arctic
614 Ocean temperatures during the Palaeocene/Eocene thermal maximum. Nature 441, 610–

613. doi:10.1038/nature04668
Stein, R., 2008. Mesozoic to cenozoic palaeoenvironmental records of high northern latitudes, in: Developments in Marine Geology. Elsevier, Amsterdam, pp. 439–496. doi:10.1016/S1572-5480(08)00007-9
Stein, R., Boucsein, B., Meyer, H., 2006. Anoxia and high primary production in the Paleogene central Arctic Ocean: First detailed records from Lomonosov Ridge. Geophys. Res. Lett. 33, 2–7. doi:10.1029/2006GL026776
Stein, R., Weller, P., Backman, J., Brinkhuis, H., Moran, K., Pälike, H., 2014. Cenozoic Arctic Ocean Climate History: Some highlights from the IODP Arctic Coring Expedition (ACEX), in: Stein, R., Blackman, D., Inagaki, F., Larsen, H.-C. (Eds.), Earth and Life Processes Discovered from Subseafloor Environment - A Decade of Science Achieved by the Integrated Ocean Drilling Program (IODP), Series Developments in Marine Geology, Vol. 7. Elsevier, Amsterdam, pp. 259–293.
von Lützow, M., Kögel-Knabner, I., Ekschmitt, K., Matzner, E., Guggenberger, G., Marschner, B., Flessa, H., 2006. Stabilization of organic matter in temperate soils: Mechanisms and their relevance under different soil conditions - A review. Eur. J. Soil Sci. 57, 426–445. doi:10.1111/j.1365-2389.2006.00809.x
Weijers, J.W.H., Schouten, S., Sluijs, A., Brinkhuis, H., Sinninghe Damsté, J.S., 2007. Warm arctic continents during the Palaeocene-Eocene thermal maximum. Earth Planet. Sci. Lett. 261, 230–238. doi:10.1016/j.epsl.2007.06.033
Weller, P., Stein, R., 2008. Paleogene biomarker records from the central Arctic Ocean (Integrated Ocean Drilling Program Expedition 302): Organic carbon sources, anoxia, and sea surface temperature. Paleoceanography 23, 1–15. doi:10.1029/2007PA001472
Westerhold, T., Röhl, U., Laskar, J., 2012. Time scale controversy: Accurate orbital calibration of the early Paleogene. Geochemistry, Geophys. Geosystems 13, 1–19. doi:10.1029/2012GC004096
Westerling, A.L., 2006. Warming and Earlier Spring Increase Western U.S. Forest Wildfire Activity 1161, 940–943. doi:10.1126/science.1128834
Wing, S.L., Currano, E.D., 2013. Plant response to a global greenhouse event 56 million years ago. Am. J. Bot. 100, 1234–1254. doi:10.3732/ajb.1200554
Wing, S.L., Harrington, G.J., Smith, F.A., Bloch, J.I., Boyer, D.M., Freeman, K.H., 2005. Transient floral change and rapid global warming at the Paleocene-Eocene Boundary. Science (80-.). 310, 993–996. doi:10.1126/science.1116913

Figures

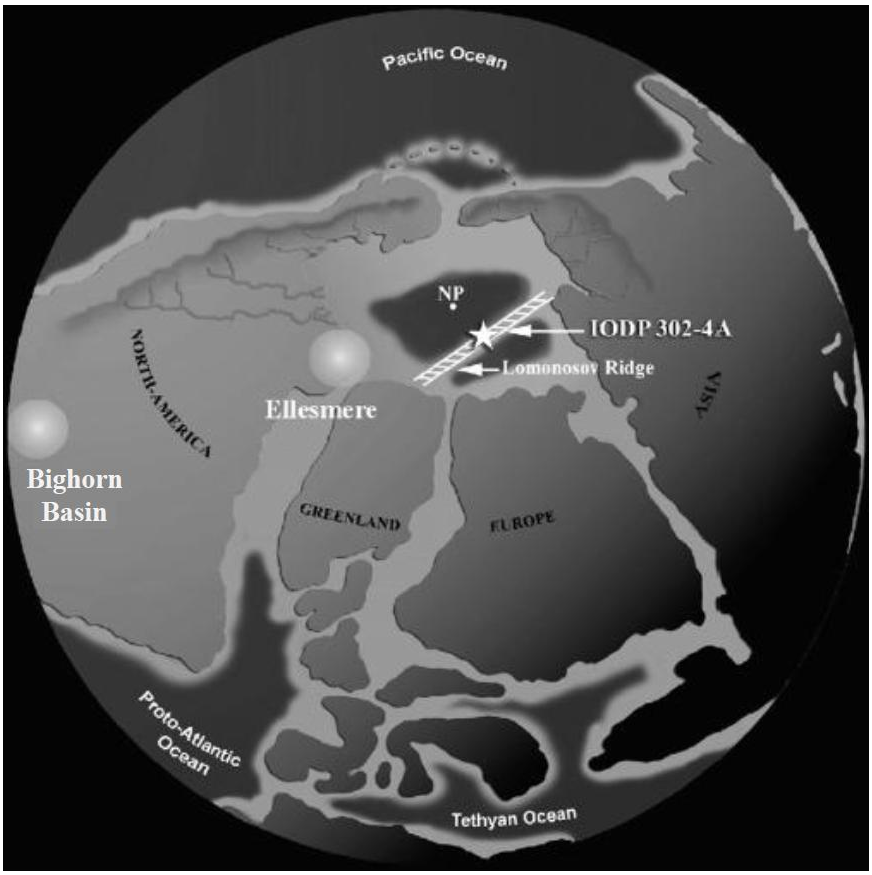

Figure 1. Paleogeographic map of the late Paleocene-early Eocene with the location of IODP Hole 302-4A marked with a star (from Weijers et al., 2007).

For reference, circles highlight the Bighorn Basin, Wyoming and Ellesmere Island (includes Axel Heiberg Island). NP is North Pole.

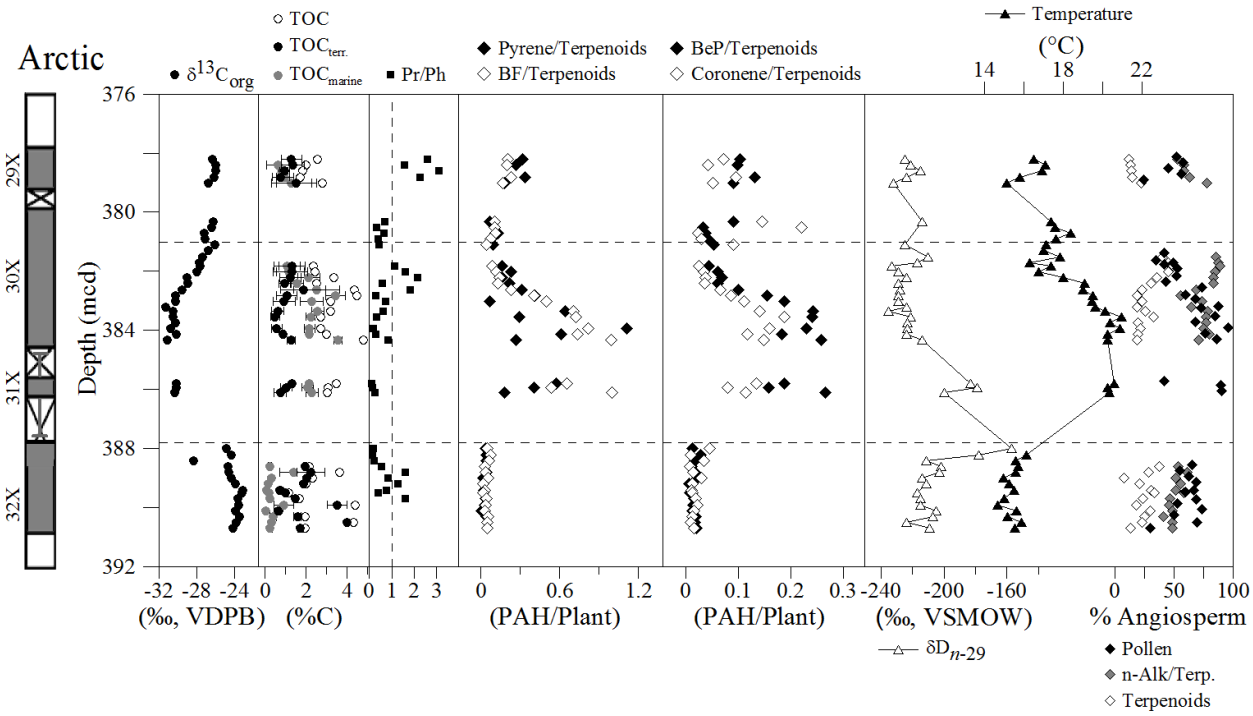

Figure 2. Depth profile of geochemical data.

Core recovery column, grey represents recovered core and "x" marks intervals without material; error bars connected to Core 31X mark the uncertainty of its stratigraphic position (Sluijs et al., 2006). Depth profile of carbon isotope ($\delta^{13}C_{org}$; black circle) and total organic carbon (TOC; white circle) (from Schouten et al., 2007)), terrestrial organic carbon ($TOC_{terr.}$; black circle); marine organic carbon (TOC_{marine}; grey circle), Pristane/Phytane (black square) and dashed line at a ratio of 1, Pyrene/Terpenoids (terpenoids are simonellite and β-amyrin derivative; black diamond), benzofluoranthene (BF)/Terpenoids (white diamond), Benzo[e]pyrene(BeP)/Terpenoids (black diamond), Coronene/Terpenoids (white diamond); δD values (white triangles with line) (Pagani et al., 2006) and air temperature based on MBT-CBT indices (black triangles with line) (Weijers et al., 2007; Peterse et al., 2012). %Angiosperm: Pollen (black diamond) and Triterpenoid/Diterpenoid (white triangle) ratios (Schouten et al., 2007); *n*-Alkanes/Diterpenoids ratio (grey diamond). Horizontal dashed lines mark the PETM interval. Horizontal bars connected to TOC represent the uncertainty in $TOC_{terr.}$ or TOC_{marine} since each was determined from an average of the BIT index and %Terrestrial Palynomorphs (from Sluijs et al. (2006)). If bar is not visible, uncertainty is less than the size of symbol.

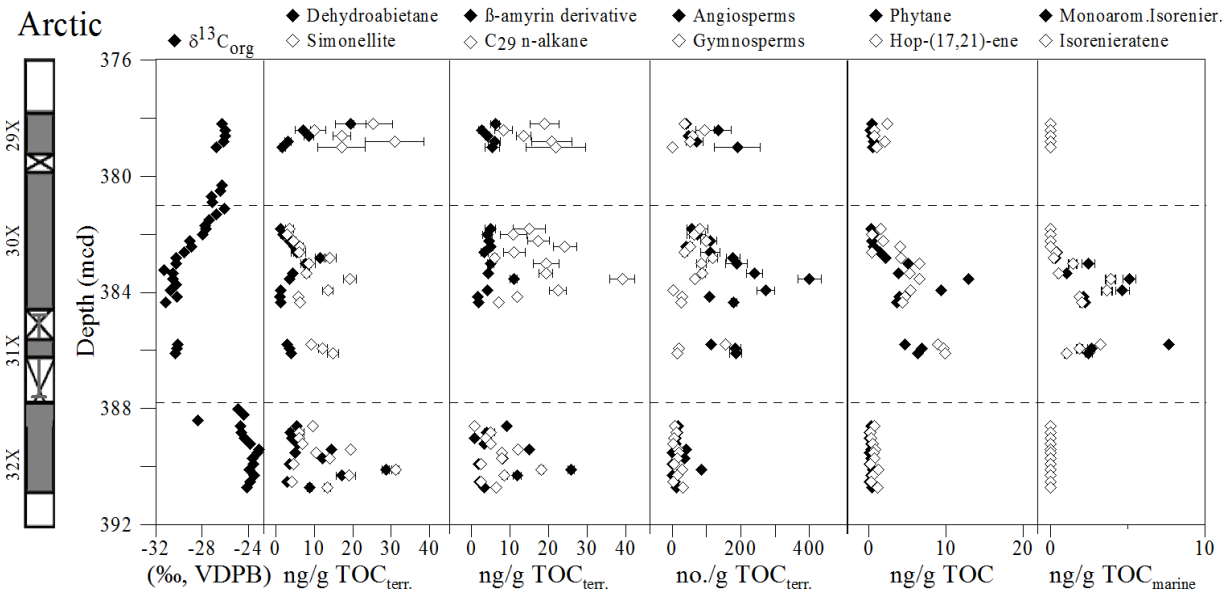

Figure 3. Depth profile of molecular compounds and pollen.

Core recovery column, where grey represents recovered core and "x" marks intervals without recovered material; error bars connected to Core 31X mark the uncertainty of its stratigraphic position (Sluijs et al., 2006). Carbon isotope values and biomarker concentrations were determined by Schouten et al. (2007). Depth profiles of organic carbon isotopes ($\delta^{13}C_{org}$; black circle), dehydroabietane (black diamond), simonellite (white diamond), β-amyrin derivative (black diamond), C_{29} *n*-alkane (white diamond), angiosperms (black diamond) and gymnosperms (white diamond) pollen abundance (number/g TOC_{terr}), phytane (black diamond), hop-(17,21)-ene (white diamond), monoaromatic derivative of isorenieratene (black diamond), isorenieratene (white diamond). Horizontal dashed lines mark the PETM interval. $TOC_{terr.}$ is the estimated terrestrial organic carbon and TOC_{marine} is the estimated marine organic carbon. Horizontal bars represent the uncertainty in $TOC_{terr.}$ or TOC_{marine} since each was determined from an average of the BIT index and %Terrestrial Palynomorphs (from Sluijs et al. (2006)). If bar is not visible, uncertainty is less than the size of symbol.

Supplemental Figures

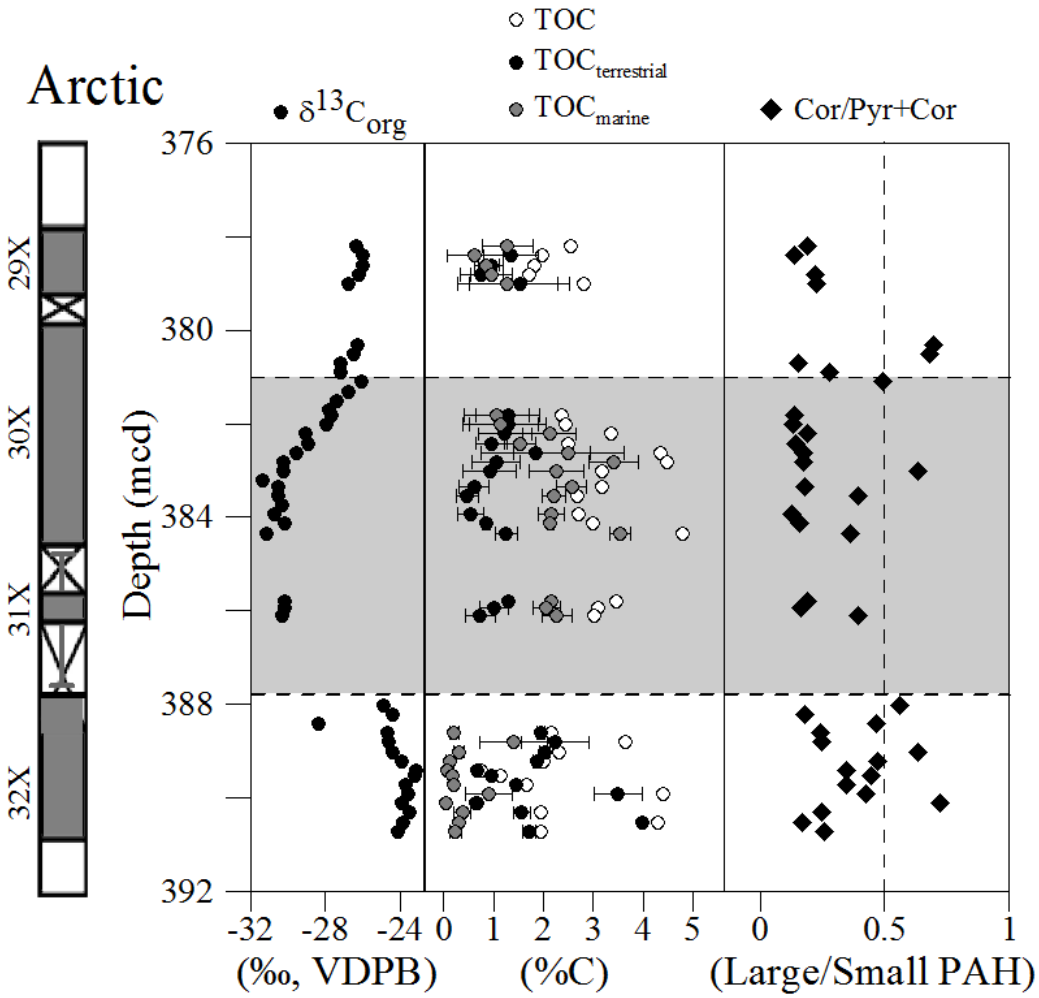

Figure S1. Depth profile from IODP Hole 302-4A of carbon isotope values, total organic carbon (TOC), and Coronene/Pyrene+Coronene ratio.

Core recovery column, where grey represents recovered core and "x" marks intervals without recovered material; error bars connected to Core 31X mark the uncertainty of its stratigraphic position (Sluijs et al., 2006). Depth profile of carbon isotope ($\delta^{13}C_{org}$; black circle), total organic

carbon (TOC; white circle) (from Schouten et al., 2007)), terrestrial organic carbon ($TOC_{terr.}$; black circle); marine organic carbon (TOC_{marine}; grey circle) values, Coronene/Pyrene+Coronene ratio (black diamond) with dashed line at a ratio of 0.5. Horizontal dashed lines mark the PETM interval. Horizontal bars represent the uncertainty in $TOC_{terr.}$ or TOC_{marine} since each was determined from an average of the BIT index and %Terrestrial Palynomorphs (from Sluijs et al. (2006)). If bar is not visible, uncertainty is less than the size of symbol.

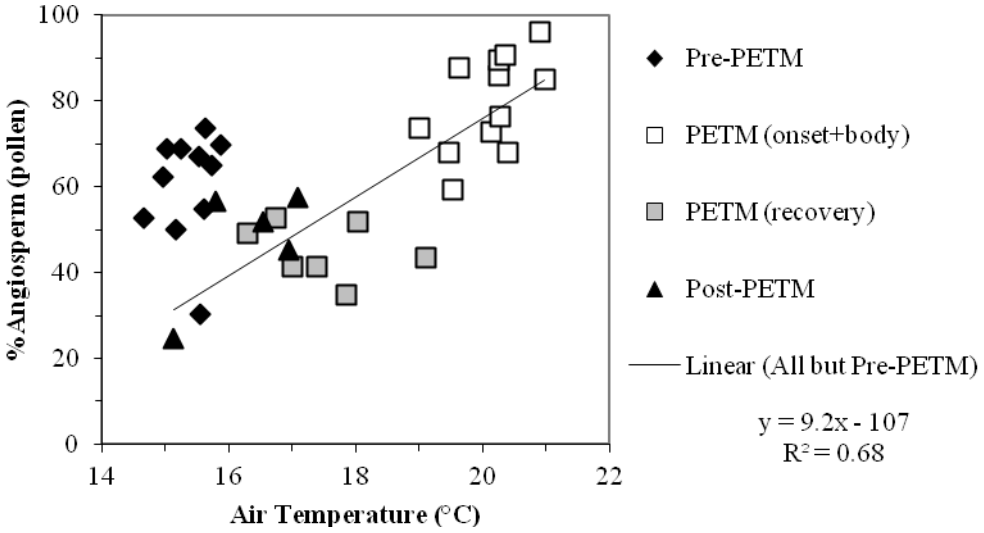

Figure S2. Correlation of percent of angiosperms (%Angiosperm) with air temperature.

Plot is based on pollen data from Sluijs et al. (2006) and air temperature (based on the MBT-CBT indices) from Weijers et al. (2007) and Peterse et al. (2012). Symbols represent: Paleocene Pre-PETM samples (solid diamond), PETM samples (square); carbon isotope excursion (CIE) onset and body (open) and CIE recovery (grey fill), Eocene Post-PETM samples (white triangle). Linear trendline for all but Pre-PETM samples (black line).

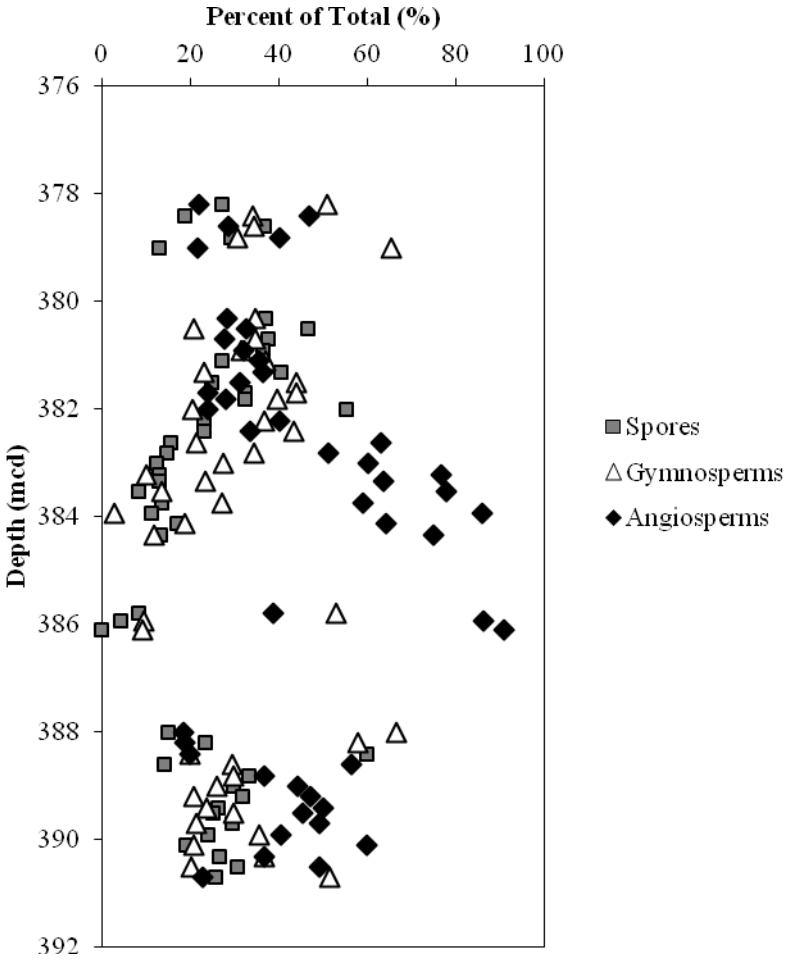

Figure S3. Relative percentage of terrestrial palynomorphs by type: spores (square); angiosperms (black diamond), gymnosperms (white triangle) (data from Sluijs et al. (2006)).

Figure 1

Click here to download Figure: Figure1.pdf

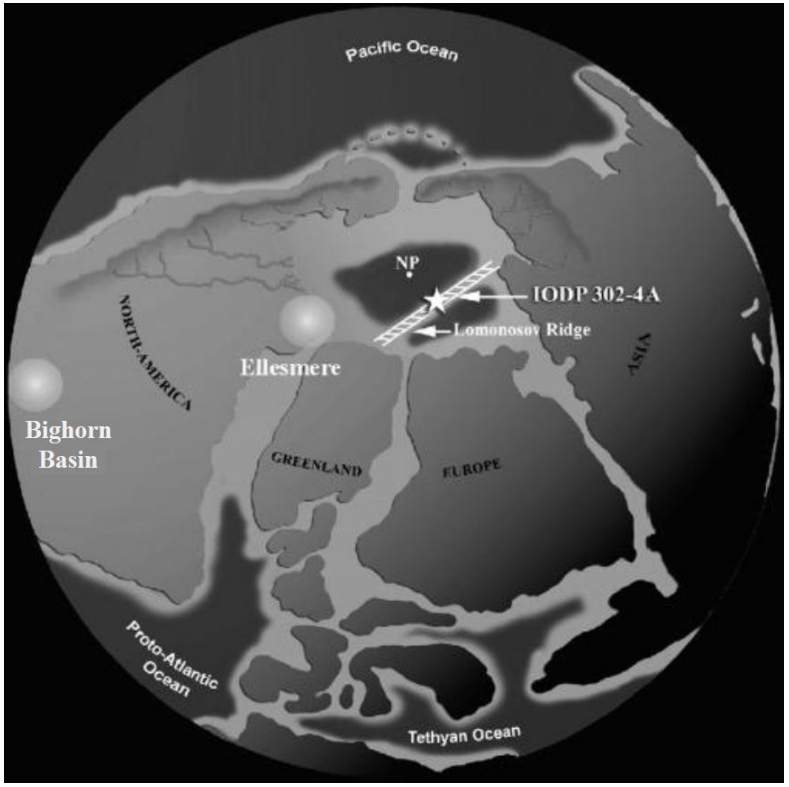

Figure 2

Click here to download Figure: Figure2.pdf

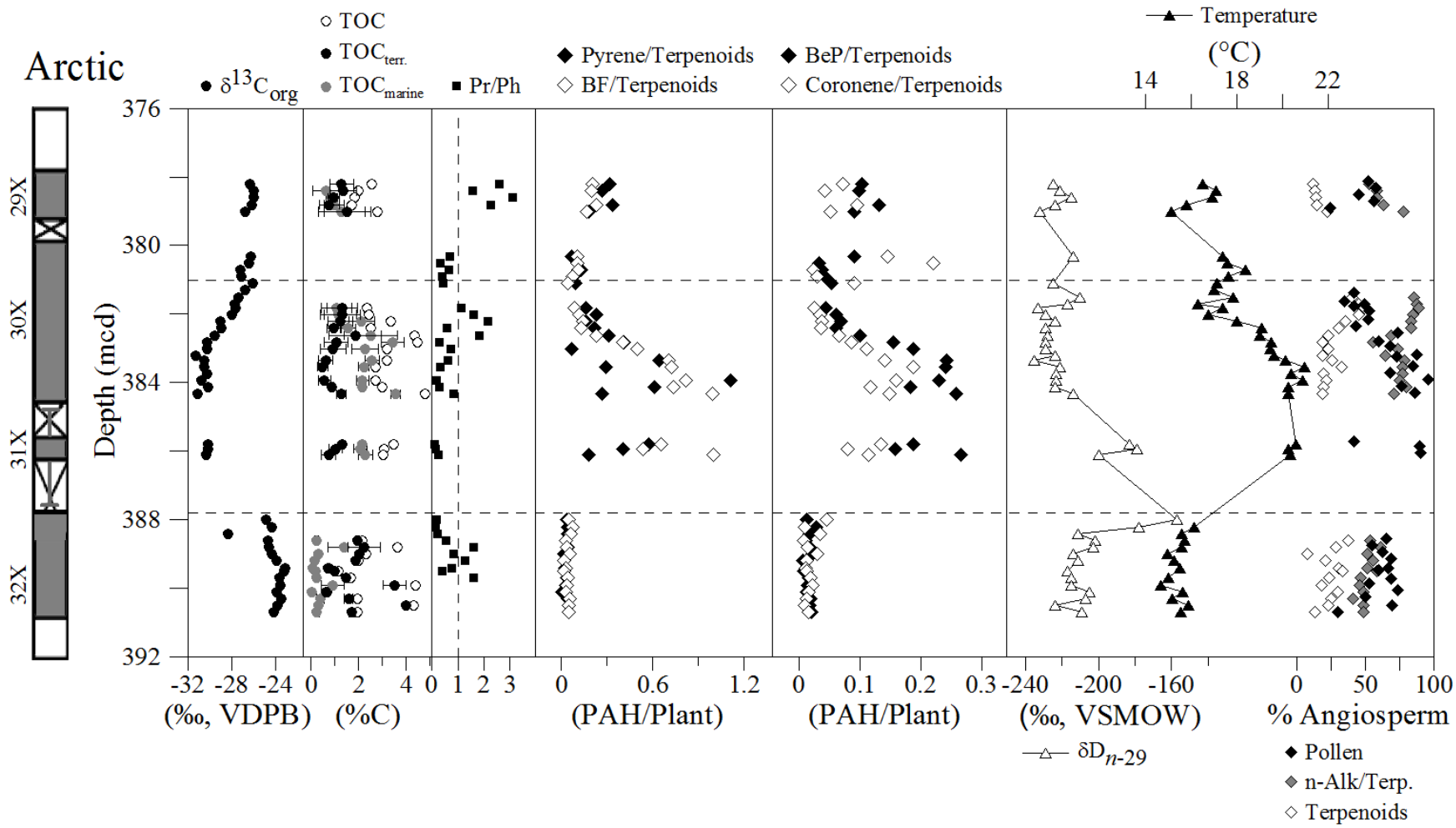

Figure 3

Click here to download Figure: Figure3.pdf

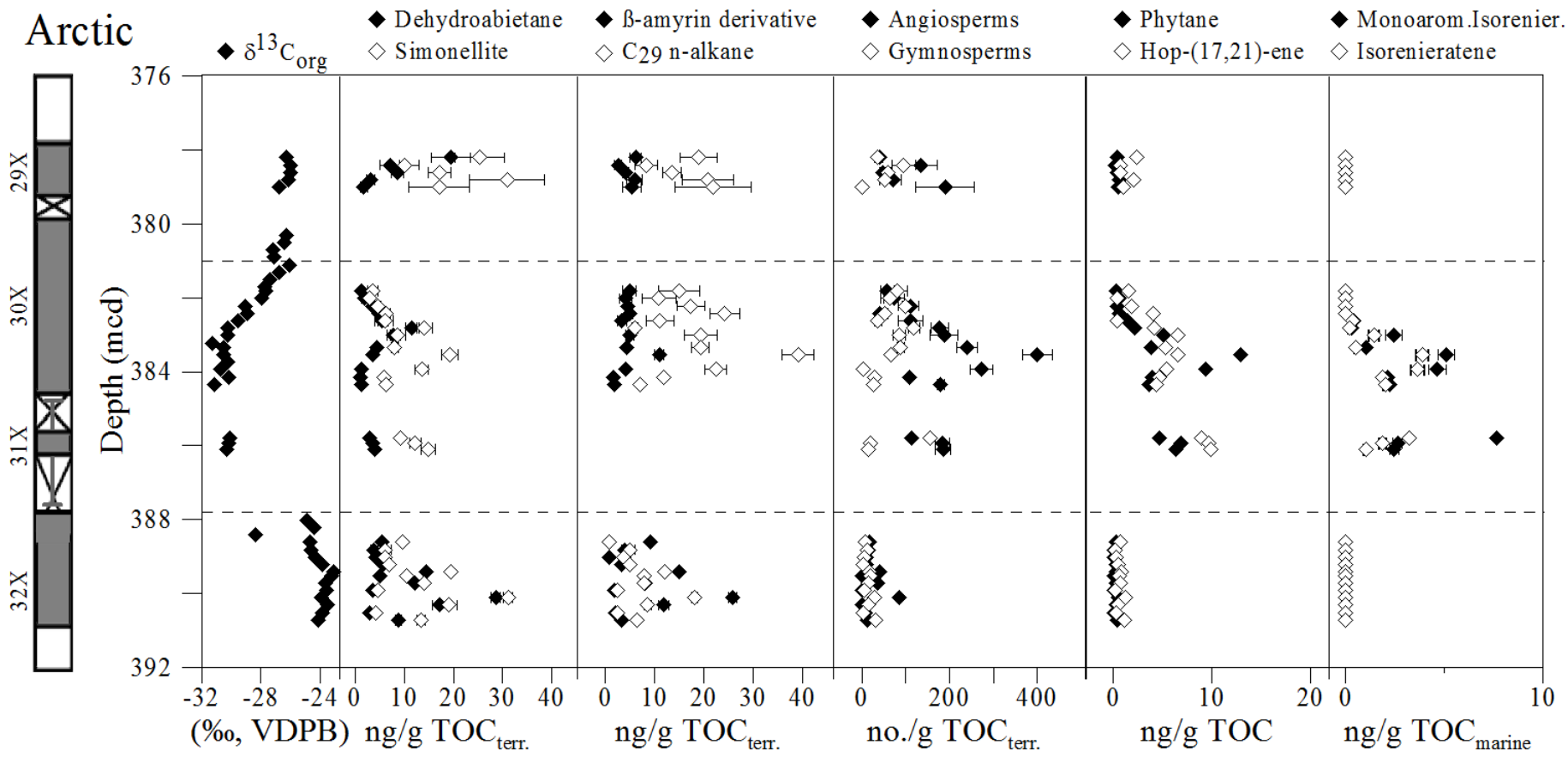

Supplemental Figure 1

Click here to download Supplementary material for online publication only: SupplementalFigure1.pdf

Supplemental Figure 2

Click here to download Supplementary material for online publication only: SupplementalFigure2.pdf

Supplemental Figure 3

Click here to download Supplementary material for online publication only: SupplementalFigure3.pdf